Spora: A Journal of Biomathematics

Volume 3 | Issue 1 Article 1

2017

The Interaction of Calcium and Metabolic Oscillations in Pancreatic β-cells

Mary Aronne
University of Maryland, Baltimore County, maronne1@umbc.edu

Samantha Clapp
Georgia College and State University, samantha.clapp@bobcats.gcsu.edu

Soohwan Jung
Edmonds Community College, s.jung8061@edmail.edcc.edu

Abigail Kramer
Kent State University, akrame13@kent.edu

William Wang
Vanderbilt University, william.wang@vanderbilt.edu

See next page for additional authors

The Interaction of Calcium and Metabolic Oscillations in Pancreatic β-cells

Cover Page Footnote
[1] Mary Aronne, Samantha Clapp, Soohwan Jung, Abigail Kramer, William Wang, Janita Patwardhan, and Bradford E. Peercy. The Interaction of Calcium and Metabolic Oscillations in Pancreatic Beta cells, Technical Report HPCF 2016 14, UMBC High Performance Computing Facility, University of Maryland, Baltimore County, 2016. [2] Richard Bertram, Leslie Satin, Min Zhang, Paul Smolen, and Arthur Sherman. Calcium and glycolysis mediate multiple bursting modes in pancreatic islets. Biophysical Journal, 87:3074 3087, 2004. [3] George Eskandar, Jennifer Houser, Ellen Prochaska, Jessica Wojtkiewicz, Terasa Lebair, and Bradford E. Peercy. Investigating how calcium diusion aects metabolic oscillations and synchronization of pancreatic beta cells. Technical Report HPCF 2015 24, UMBC High Performance Computing Facility, University of Maryland, Baltimore County, 2014. [4] Christopher P. Fall. Computational Cell Biology. Springer, 2002. [5] Samuel Khuvis, Matthias K. Gobbert, and Bradford E. Peercy. Time-stepping techniques to enable the simulation of bursting behavior in a physiologically realistic computational islet. Mathematical Biosciences, 263:1 17, 2015. [6] K Tsaneva-Atanasova, CL Zimliki, R Bertram, and A Sherman. Diusion of calcium and metabolites in pancreatic islets: killing oscillations with a pitchfork. Biophysical Journal, 90:3434 3046, 2006. [7] Margaret Watts, Bernard Fendler, Matthew J. Merrins, Leslie S. Satin, Richard Bertram, and Arthur Sherman. Calcium and metabolic oscillations in pancreatic islets: Who's driving the bus? SIAM Journal on Applied Dynamical Systems, 13(2):683 703, 2014.

Authors
Mary Aronne, Samantha Clapp, Soohwan Jung, Abigail Kramer, William Wang, Janita Patwardhan, Bradford E. Peercy, and Arthur Sherman

Intercollegiate Biomathematics Alliance

SPORA
A Journal of Biomathematics

ISSN 2473-3067 (Print)
ISSN 2473-5493 (Online)

The Interaction of Calcium and Metabolic Oscillations in Pancreatic β-cells

Mary Aronne[1], Samantha Clapp[2], Soohwan Jung[3], Abigail Kramer[4], William Wang[5], Janita Patwardhan[1], Bradford E. Peercy[1,*], Arthur Sherman[6]

[*]Correspondence:
Dr. Bradford E. Peercy,
Dept. of Mathematics and Statistics, University of Maryland, Baltimore County,
1000 Hilltop Cir, Baltimore,
MD 21250, USA
bpeercy@umbc.edu

Abstract

Diabetes is a disease characterized by an excessive level of glucose in the bloodstream, which may be a result of improper insulin secretion. Insulin is secreted in a bursting behavior of pancreatic β-cells in islets, which is affected by oscillations of cytosolic calcium concentration. We used the Dual Oscillator Model to explore the role of calcium in calcium oscillation independent and calcium oscillation dependent modes and the synchronization of metabolic oscillations in electrically coupled β-cells. We implemented a synchronization index in order to better measure the synchronization of the β-cells within an islet, and we studied heterogeneous modes of coupled β-cells. We saw that increasing calcium coupling or voltage coupling in heterogeneous cases increases synchronization; however, in certain cases increasing both voltage and calcium coupling causes desynchronization. To better represent an islet, we altered previous code to allow for a greater number of cells to be simulated.

Keywords: pancreatic β-cells, islet, calcium, metabolic oscillations, Dual Oscillator Model

1 Introduction

Insulin is a hormone secreted by pancreatic β-cells that manages blood plasma glucose levels. Improper insulin secretion can result in chronically elevated levels of glucose in the bloodstream in a disease known as diabetes. Diabetes can lead to kidney failure, blindness, limb amputation, cardiovascular disease, and death [8]. There are two types of diabetes: Type I involves an autoimmune destruction of β-cells, which results in a complete absence of insulin. Type II involves a deficiency of insulin caused by insulin resistance as well as a failure of β-cells to produce enough insulin to compensate. Type II is the more common form of diabetes, with a rising number of cases concentrated in industrialized countries [8]. The rise in diabetes has driven research to better understand β-cells.

In Zhang et al. [18], pulsatile insulin, where insulin is presented in brief pulses as opposed to a continuous manner, is characterized. It results from bursts of calcium releasing vesicles containing insulin. Pulsatile insulin is known to exist in humans and many mammals [10, 15] and to be more effective on its target tissues [13, 5, 12], while patients with Type II diabetes exhibit disrupted pulsatility [2, 14]. The period of these oscillations varies but is generally around 5 minutes [2, 4]. The calcium bursts responsible for releasing the insulin-containing vesicles are known to derive from ionic channels, cellular stores, and metabolic dynamics and demands on the cell as reviewed in [4]. However, some details of metabolic demands and oscillations interplay with calcium dynamics in whole islets are not well understood. We address this with a mathematical model.

To model a β-cell, we use the Dual Oscillator Model (DOM), a system of ordinary differential equations which consists of the interacting electrical, glycolytic, and mitochondrial components, based originally on the Hodgkin-Huxley Model with significant revisions made for our system, including the FitzHugh-Nagumo Reduction [8]. The DOM has already been used to address questions about situations under which metabolic oscillations occur, especially focusing on the effect of calcium oscillations as newer versions of the model suggest that calcium plays a bigger role in metabolic oscillations, where certain modes require the presence of calcium oscillations for metabolic oscillations to occur. The model in Watts et al. [17] has been adapted to work as a multi-cell islet model as in Eskandar et al. [6]. We will consider how dynamics change when working with islet oscillations dependent on calcium oscillations.

The bifurcation structure of the DOM has been studied to examine how both the electrical oscillator and

[1]Department of Mathematics and Statistics, UMBC, [2]Department of Mathematics, Georgia College and State University, [3]Department of Mathematics, Edmonds Community College, [4]Department of Mathematical Sciences, Kent State University, [5]Department of Mathematics, Vanderbilt University, [6]Laboratory of Biological Modeling, National Institutes of Health

the glycolytic oscillator work together, and we will rely heavily on the two-parameter bifurcation diagram in the J_{GK}-Ca_c plane based on the isolated glycolytic oscillator system to obtain our results. We have a model and methods to further understand what causes oscillations of β-cells in pancreatic islets to synchronize.

Our research focuses on understanding β-cells by investigating calcium oscillation independent (CaI) and calcium oscillation dependent (CaD) modes. We do this through exploring the effects of voltage and calcium coupling as well as different types of heterogeneous cellular bursting arrangements on the synchronization of cells in these modes. We have arranged our report as follows: In Section 2 there is a brief overview of the physiology of β-cells as well as the Dual Oscillator Model. The methodology is described in Section 3 and the results are described in Section 4. The conclusions of our research are drawn in Section 5.

2 Background

2.1 Physiology

In the pancreas, the endocrine cells are found in clusters called islets of Langerhans [8]. The islet primarily consists of α-, β-, and δ-cells; the β-cells are responsible for insulin secretion. The process of insulin secretion begins when glucose enters a β-cell. Glycolysis starts, during which adenosine diphosphate (ADP) is converted to adenosine triphosphate (ATP). The ratio of ATP to ADP increases, causing the ATP dependent potassium channels (K_{ATP}) to close and the β-cell to depolarize. As a result, the calcium (Ca^{2+}) channels open, allowing Ca^{2+} to flow into the cytoplasm from the outside of the cell. The increase in Ca^{2+} triggers the endoplasmic reticulum (ER) to open its large Ca^{2+} store, leading to a higher concentration of Ca^{2+} in the cell. Due to this greater concentration, insulin is released into the bloodstream through exocytosis. The ATP/ADP ratio is restored by exocytosis and other cell functions, such as the calcium pump that expels excess Ca^{2+}, lowering the concentration. The K_{ATP} channel is reopened and the cell is repolarized, resetting the β-cell.

The process of the calcium channels opening and closing results in calcium oscillations, whereas the flow of ions in and out of the cell lead to voltage oscillations. Furthermore, the ATP oscillations depend on negative feedback from the Ca^{2+} [11]. During the process of glycolysis, there is a positive feedback loop of fructose 1,6-bisphosphate (FBP) on phosphofructokinase (PFK) causing the production of more FBP until fructose 6-phosphate (F6P) is depleted, which causes PFK activity to stop until F6P levels recover. This process causes metabolic oscillations. There are different values of the flux of glucokinase (J_{GK}) that determine whether a cell is CaI or CaD. If it depends on the calcium oscillation levels, it is CaD, and if it does not depend on the calcium oscillation levels, it is CaI. The range of CaD is $0.00 \leqslant J_{GK} \leqslant 0.01$ and $J_{GK} \geqslant 0.176$. The range of CaI is $0.045 \leqslant J_{GK} \leqslant 0.15$, and these parameter values are used for the β-cells [17]. Ca^{2+} links the electrical and metabolic oscillations that are exhibited by β-cells in response to elevated glucose levels in the bloodstream. Together these two oscillations regulate the secretion of insulin by the β-cells. A complete oscillation is considered a *burst*, representing one cycle of insulin secretion. β-cells can be classified into two categories, slow and fast, based upon their bursting periods. Slow bursting β-cells burst approximately every four to six minutes. Fast bursting β-cells burst approximately every ten seconds [7]. In islets however, there is a mix of differently bursting cells called heterogeneity. The timing of the insulin secretion process is dependent on the (J_{GK}) value of the cell.

The β-cells do not act independently to release insulin. They are connected by gap junctions, which are proteins split between the cell membranes that allow small molecules to travel from cell to cell. Gap junctions impact the voltage between cells as well as Ca^{2+} concentration in each cell. A transmembrane current is created across the gap junction due to the flow of ions between cells [8]. As the process of insulin secretion happens for one cell, it is signaled to the connecting cells and the bursting is synchronized [7].

Insulin secretion is oscillatory in healthy cells; however, these oscillations often are not observed in pre-diabetic subjects. It is possible that the lack of oscillations are connected with dysynchronization of β-cells in an islet.

2.2 Dual Oscillator Model

The Dual Oscillator Model (DOM) [17] represents the process of insulin secretion for a single β-cell by seven differential equations (1a)–(1g) consisting of three components: electrical, mitochondrial, and glycolytic. The DOM is given by

$$\frac{dV}{dt} = -\frac{I_K + I_{Ca} + I_{K(Ca)} + I_{K(ATP)}}{C_m} \tag{1a}$$

$$\frac{dn}{dt} = \frac{n_\infty(V) - n}{\tau_n} \tag{1b}$$

$$\frac{d[Ca]}{dt} = f_{cyt}(J_{mem} + J_{er}) \tag{1c}$$

$$\frac{d[Ca_{er}]}{dt} = -\sigma_V f_{er} J_{er} \tag{1d}$$

$$\frac{d[ADP]}{dt} = J_{hyd} - \delta J_{ANT} \tag{1e}$$

$$\frac{d[G6P]}{dt} = k(J_{GK} - J_{PFK}) \tag{1f}$$

$$\frac{d[FBP]}{dt} = k(J_{PFK} - \tfrac{1}{2}J_{GPDH}). \tag{1g}$$

Equations (1a)–(1d) contain the electrical model, Equation (1e) describes the cell's mitochondrial activity, and Equations (1f) and (1g) represent glycolytic activity. Note that $[\cdot]$ represents the concentration of particular molecules. The seven state variables are membrane potential (V), the activation variable for the voltage dependent K channel (n), and the concentrations of the free cytoplasmic calcium ($[Ca]$), the free cytoplasmic calcium in the ER ($[Ca_{er}]$), ADP ($[ADP]$), the glucose 6-phosphate in the cell ($[G6P]$), and FBP ($[FBP]$). Also, J_x serves to show flux where $x \in \{mem, er, hyd, ANT, GK, PFK, GPDH\}$.

In Equation (1a), I_i indicates the ionic currents through the specific channels where $i \in \{K, Ca, K(Ca), K(ATP)\}$. Note that I_K and I_{Ca} are voltage dependent, $I_{K(Ca)}$ is Ca^{2+}-activated, and $I_{K(ATP)}$ is sensitive to the ATP/ADP ratio. The variable C_m represents the membrane capacitance. In Equation (1b), τ_n is a time constant.

The equations for the currents, which use Ohm's law and form the basis for Equation (1a), are given by

$$I_K = \bar{g}_K n(V - V_K) \tag{2a}$$

$$I_{Ca} = \bar{g}_{Ca} m_\infty (V - V_{Ca}) \tag{2b}$$

$$I_{K(Ca)} = g_{K(Ca)}(V - V_K) \tag{2c}$$

$$I_{K(ATP)} = g_{K(ATP)}(V - V_K). \tag{2d}$$

Note that g_i is conductance whereas $\bar{g}_i$ represents the maximal conductance for the respective current.

The activation variables n and m are given by

$$n_\infty(V) = \frac{1}{1 + e^{-(16+V)/5}} \tag{3a}$$

$$m_\infty(V) = \frac{1}{1 + e^{-(20+V)/12}}. \tag{3b}$$

The K(Ca) conductance in (4a) is given by an increasing sigmoidal function of the Ca^{2+} concentration and the K(ATP) conductance in (4b) is dependent on the ADP and ATP concentrations, where the conductance function O_∞ is given by the Magnus-Keizer expression [3], as shown by

$$g_{K(Ca)} = \bar{g}_{K(Ca)} \left(\frac{Ca^2}{K_D^2 + Ca^2} \right) \tag{4a}$$

$$g_{K(ATP)} = \bar{g}_{K(ATP)} O_\infty(ADP, ATP). \tag{4b}$$

The concentration of calcium in Equation (1c) uses the fraction of free to total cytosolic Ca^{2+} (f_{cyt}) along with Equations (5a) through (5d). The flux equations are given by

$$J_{mem} = -(\alpha I_{Ca} + k_{PMCA}[Ca]) \tag{5a}$$

$$J_{er} = J_{leak} - J_{SERCA} \tag{5b}$$

$$J_{leak} = p_{leak}([Ca_{er}] - [Ca]) \tag{5c}$$

$$J_{SERCA} = k_{SERCA}[Ca]. \tag{5d}$$

These equations describe the flux of Ca^{2+} across the membrane (J_{mem}), the flux of Ca^{2+} out of the endoplasmic reticulum (J_{er}), leakage permeability (p_{leak}), and SERCA pump rate (k_{SERCA}). In Equation (5a), α converts current to flux and k_{PMCA} is the Ca^{2+} pump rate. In our reduced model, only the leakage (J_{leak}) leads to flux out of the ER, and only the SERCA pumps (J_{SERCA}) lead to Ca^{2+} flux into the ER.

Returning to Equation (1d), we have $[Ca_{er}]$ determined by the volume fraction of the relationship between the ER and the cytoplasm (σ_V), the flux across the ER (J_{er}), and the fraction of free to total cytosolic Ca^{2+} in the ER (f_{er}).

The concentration of ADP, representing the mitochondrial component, is determined by the flux through the ATP hydrolysis (J_{hyd}) and the flux through the mitochondrial translocator (J_{ANT}) which are given by

$$J_{ANT} = p19 \frac{ATP_m/ADP_m}{ATP_m/ADP_m + p20} \exp\left(\frac{F\psi_m}{2RT}\right) \tag{6a}$$

$$J_{hyd} = (k_{hyd} Ca_c + J_{hyd,SS}) ATP_c. \tag{6b}$$

In Equations (6a) and (6b), F is Faraday's constant, R is the universal gas constant, T is the temperature, and ψ_m is the mitochondrial membrane potential, which is taken to be constant. The calcium-dependent component of hydrolysis is given by k_{hyd}, and $J_{hyd,SS}$ is the basal level of hydrolysis. Thus, it can be seen from (6b) that Ca_c influences the rate of glycolysis [17].

Regarding the glycolytic component, Equation (1f) shows ([G6P]), produced in the first step of glycolysis, given by the flux through phosphofructokinase (J_{PFK}) and the flux through glucokinase (J_{GK}). In Equation (1g), J_{PFK} and the flux through glyceraldehyde 3-P dehydrogenase (J_{GPDH}) determine [FBP]. The glycolytic component is capable of generating slow oscillations without calcium oscillations because of negative feedback from G6P and positive feedback by FBP.

2.3 Coupling

Coupling of N^3 cells is considered to better understand the way β-cells interact in islets through gap junctions. To couple multiple cells in an islet, we created a diagonal coupling matrix G, which connects the voltages and

calcium concentrations between a cell and its neighboring cells. We construct a vector,

$$y = \begin{bmatrix} V_i \\ n_i \\ [Ca]_i \\ [Ca_{ER}]_i \\ [ADP]_i \\ [G6P]_i \\ [FBP]_i \end{bmatrix}, \text{ where } i = 1 \text{ to } N, \tag{7}$$

that contains these values for all of the cells. We now define our system of ODEs to be

$$\frac{dy}{dt} = f(t, y) + Gy, \tag{8}$$

where $f(t, y)$ encompasses the happenings inside each cell taken from the DOM and Gy accounts for the adjusted behavior of the β-cells due to coupling.

3 Numerical Methods

The DOM can be examined two ways: as a single cell model and as an islet model. The single cell model shows how one β-cell reacts to electrical and metabolic oscillations represented in Equations (1a)–(1g). The islet model replicates this single cell model for N^3 cells then uses the coupling matrix G to consider how the cells interact. Both models are based on Matlab files used in previous work at University of Maryland, Baltimore County High Performance Computing Facility [7]. This file was adapted from Bertram's `XPPAUT` file that implemented the DOM [3].

3.1 Islet Model

The islet is modeled as a cube of $N \times N \times N$ cells with indexing (i, j, k). Note that this means our ODE system becomes $7N^3$ differential equations. For computational purposes, the values associated with each cell are stored in a vector y, in Equation (7). The indexing is given as $l = i + N(j-1) + N^2(k-1)$ to access the $(i, j, k)^{\text{th}}$ element in y. To compute the impact of coupling on each cell, the C matrix shows the influence of the surrounding cells on each individual cell. The matrix C consists of coupling coefficient values that are modified to account for the chosen coupling values in C'. The matrix G is a block diagonal matrix, with each block on the diagonal containing C'. Each row represents the effects of connecting cells to one cell. If the m^{th} and n^{th} cells are not connected, then the (m, n) and (n, m) entries of the matrix will be zero; if they are connected, the entries will be their coupling relation. The diagonal of matrix C is the number of neighboring cells multiplied by the coupling value, g. More information on the coupling matrix can be found in [9].

To accurately represent an islet, the initial values of each cell are taken from a normal distribution around the average value with standard deviation 20% of that average value. This allows the initial values of each cell to be chosen within a certain range of the mean to see how the cell bursts synchronize. We take into account the heterogeneity of an islet and use three different patterns as seen in Figures 1a, 1b, and 1c. The equal pattern in Figure 1a alternates between two J_{GK} values from cell to cell. In Figure 1b, we see a layers pattern where each row alternates the J_{GK} values. The last pattern we model is called a *layered split pattern* that alternates between half rows of J_{GK} values seen in Figure 1c. Within these patterns, we use various combinations of J_{GK} values in CaD and CaI ranges.

3.2 Optimizing the Numerical Method

To obtain numerical solutions for the DOM, we choose the built-in Matlab solver `ode15s`, which can solve stiff differential equations in the form $My' = F(t, y)$. It effectively uses a mass symbolic Jacobian matrix obtained directly from the DOM code through the streamlined means of Matlab's Automatic Differentiation. We implement a modified version of `ode15s` to optimize runtime and memory usage specifically for the DOM [9].

For simulations of a large N or high end time, the output is too large to write a MAT-file. To overcome this issue, we add a loop into the code that can run the simulation for a given amount of time and save the results in a MAT-file. Then the end value is taken as the new initial condition and the simulation is run for the next time period, saving these results in a new MAT-file. We call this loop the Time Interval Loop (TIL).

3.3 Synchronization Index

In order to quantitatively measure the level of synchronization for each simulation, we write code to output the synchronization index of V, [Ca], and [FBP] traces. To weigh the stiff and nonstiff regions of the oscillations equally in the index, we interpolate the data from the simulation using a time vector with equal spacing of 36ms per entry. A Pearson correlation runs on the matrix containing all the V, [Ca], or [FBP] traces per simulation. We use the built-in Matlab function, `corr`, for the Pearson correlation. The $(i, j)^{\text{th}}$ entry of the resulting coefficient matrix is the Pearson coefficient for the i^{th} and j^{th} traces. We determine the index by taking the minimum average value of the rows. For this index we choose for what time period of each simulation to run the correlation. Since we are considering what pattern the simulation settle into, we typically run our SI on the last fifteen minutes of the simulation.

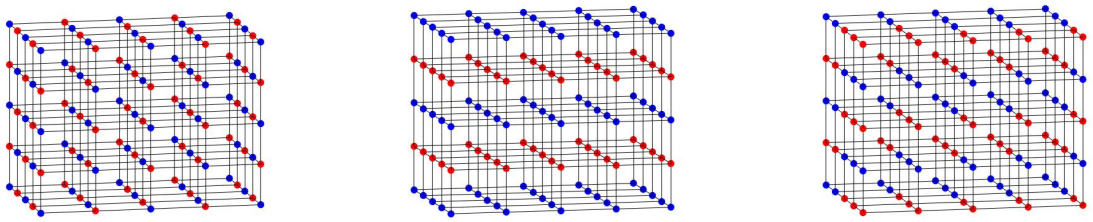

(a) Equal-50-Percent (b) Layers (c) Layered-split

Figure 1: Three different heterogeneity patterns where red and blue represent two different J_{GK} values.

4 Results

Our simulations examine the behavior of voltage, calcium, and FBP under varying parameters and between heterogeneous groups of cells representing an islet. Our results show simulations of varying J_{GK} values in the CaI, CaD, and mixed CaI and CaD ranges, as well as varying levels of calcium coupling and voltage coupling. The calcium coupling values are chosen from the range of no coupling to $0.045\,\mathrm{ms}^{-1}$, from initial tests that showed no change in synchronization when $g_{Ca} > 0.045\,\mathrm{ms}^{-1}$. The voltage coupling values are chosen to be 0, 5, and 10 pS, from initial tests which showed no significant change in synchronization with $g_V > 10\,\mathrm{pS}$.

4.1 Coupling Trends

We consider coupling in the CaD and CaI modes. In Figure 2, we consider CaI mode with a 3×3×3 islet starting from perturbed initial conditions of identical β-cells without coupling in calcium. There are two different voltage coupling strengths, 5 pS in Figure 2a and 10 pS in Figure 2b. We show calcium, voltage and FBP in time. As voltage coupling increases, synchronization modestly increases in all three variables. In Figure 3 we alter the J_{GK} value to a CaD mode. Here increasing voltage coupling seems to increases synchronization much more quickly and completely compared to the CaI mode in Figure 2. When calcium coupling values are modest ($<0.045\,\mathrm{ms}^{-1}$), there is greater synchronization as the calcium coupling values increase in both CaI, Figure 4, and CaD, Figure 5, modes, though there appears to be some variation on the fastest (ms) time scale.

When calcium coupling values are less than $0.045\,\mathrm{ms}^{-1}$, there is greater synchronization as the calcium values increase in both CaD and CaI modes as shown by Figures 4 and 5.

4.2 Heterogeneity

We test three different types of heterogeneity patterns with various pairs of J_{GK} values and various calcium and voltage coupling values. We find the differences between the three heterogeneity patterns to be small. For example in Figure 6 with voltage coupling of 5 pS, without calcium coupling, and with two-cell modes, one in CaD mode and one in CaI mode, the orientation of the cell modes has little impact on the synchronization. Similarly, in Figure 7 without voltage coupling, with calcium coupling of $0.045\,\mathrm{ms}^{-1}$, and with two-cell modes, one in CaI low mode and one in CaI high mode, the orientation of the cell modes again has little impact on the synchronization. Consequently for subsequent simulations we consider only the equal-50-percent orientation of the islet.

4.3 Synchronization

In order to quantify synchronization, we create a plot of the synchronization index (SI) for a set of simulations with varying parameters. Simulations are run with either the same or perturbed initial conditions as well as for a time period of one or two hours. Note that we apply the SI to the last fifteen minutes of each simulation. Each chart consists of twelve scatter plots with each plot representing a different voltage and calcium coupling combination. The x-axis shows the pairs of J_{GK} values while the y-axis represents the SI values. To represent the SI values of voltage, calcium, and FBP per simulation, each point is given a certain shape and color, voltage synchronization is a pink triangle, calcium synchronization a green circle, and FBP synchronization a blue X. An SI value of one represents complete synchronization.

4.3.1 Synchronization Index Charts

In the synchronization index chart, we can see the trends as we change parameters. Each column of graphs represents a specific voltage coupling, which increases from left to right. Rows of graphs represent a given calcium coupling increasing from top to bottom. The first three

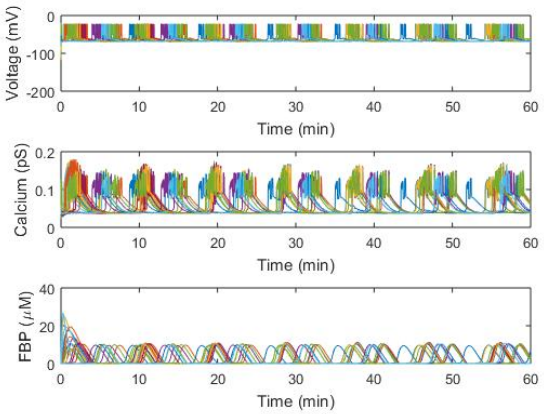

(a) $g_v = 5\,\mathrm{pS}$

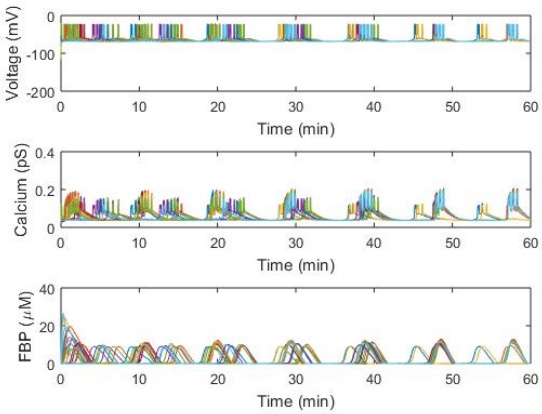

(b) $g_v = 10\,\mathrm{pS}$

Figure 2: CaI runs with a J_{GK} value of $0.095\,\mu\mathrm{M}{\cdot}\mathrm{ms}^{-1}$, a $3{\times}3{\times}3$ block of cells, homogeneous, $g_{Ca} = 0\,\mathrm{ms}^{-1}$ and the initial conditions perturbed.

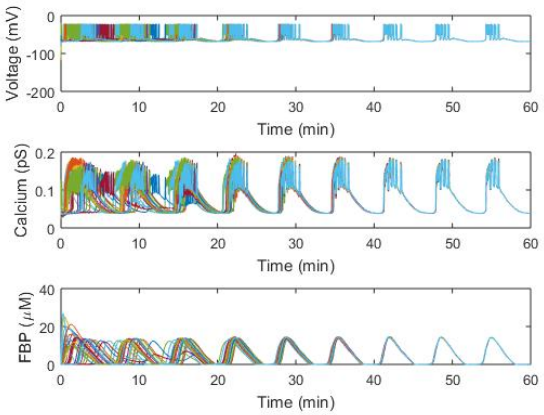

(a) $g_v = 5\,\mathrm{pS}$

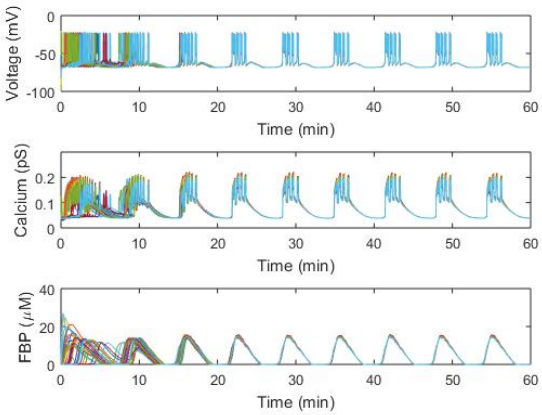

(b) $g_v = 10$

Figure 3: CaD runs with a J_{GK} value of $0.18\,\mu\mathrm{M}{\cdot}\mathrm{ms}^{-1}$, a $3{\times}3{\times}3$ block of cells, homogeneous, $g_{Ca} = 0\,\mathrm{ms}^{-1}$ and the initial conditions perturbed.

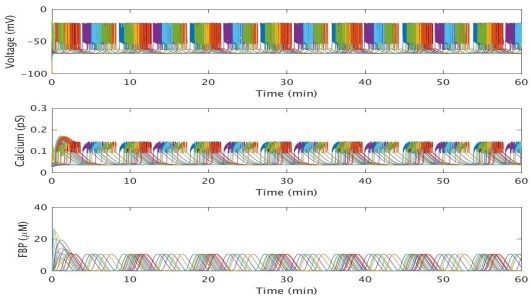

(a) $g_{ca} = 0.000009\,\mathrm{ms}^{-1}$

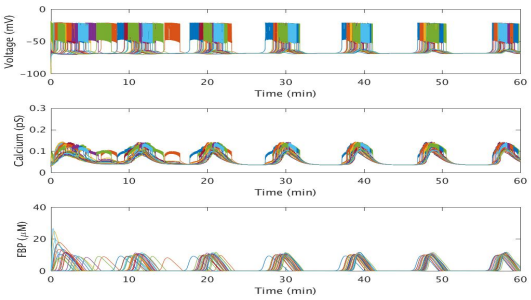

(b) $g_{ca} = 0.0018\,\mathrm{ms}^{-1}$

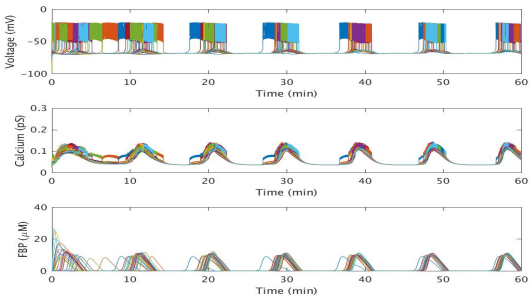

(c) $g_{ca} = 0.0036\,\mathrm{ms}^{-1}$

Figure 4: CaI runs with a J_{GK} value of $0.095\,\mu\mathrm{M}{\cdot}\mathrm{ms}^{-1}$, with a $3{\times}3{\times}3$ block of cells, are homogeneous, $g_v = 0\,\mathrm{pS}$, and the initial conditions perturbed.

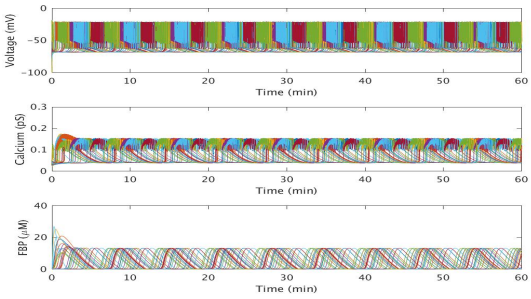

(a) $g_{ca} = 0.000009\,\mathrm{ms}^{-1}$

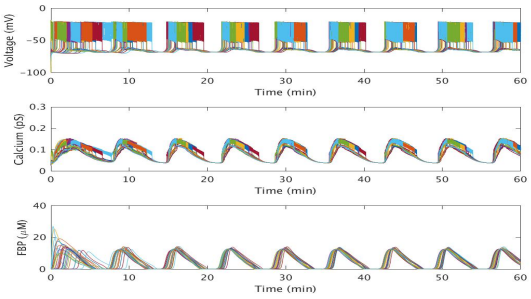

(b) $g_{ca} = 0.0018\,\mathrm{ms}^{-1}$

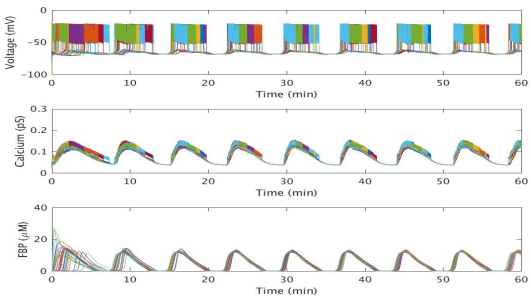

(c) $g_{ca} = 0.0036\,\mathrm{ms}^{-1}$

Figure 5: CaD runs with a J_{GK} value of $0.18\,\mu\mathrm{M}{\cdot}\mathrm{ms}^{-1}$, with a $3{\times}3{\times}3$ block of cells, are homogeneous, $g_v = 0\,\mathrm{pS}$, and the initial conditions perturbed.

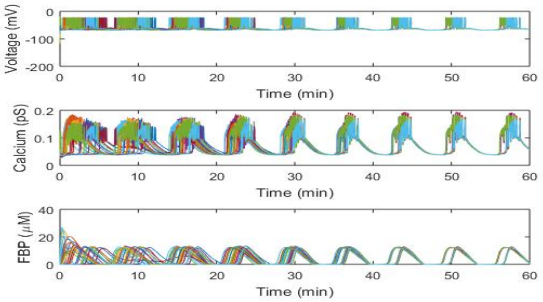

(a) Equal-50-percent

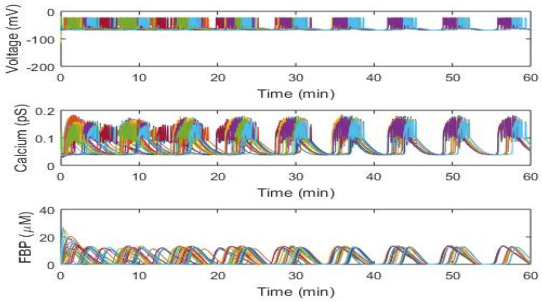

(b) Layers

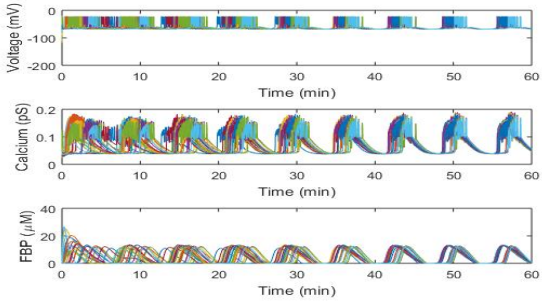

(c) Layered-split

Figure 6: Mixed CaD and CaI with J_{GK} values of 0.14 and 0.18 µM·ms^{-1}, with a 3×3×3 block of cells, $g_v = 5$ pS, $g_{Ca} = 0$ ms^{-1}, and the initial conditions perturbed.

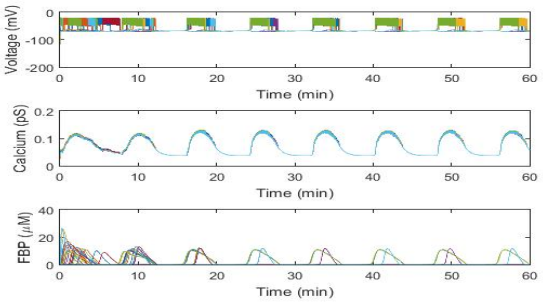

(a) Equal-50-percent

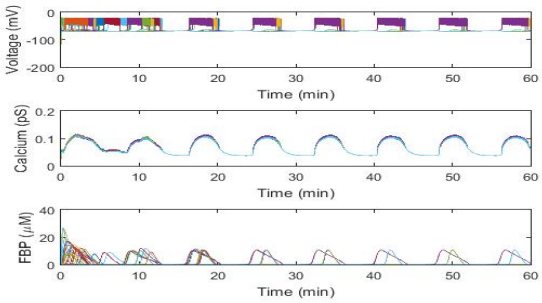

(b) Layers

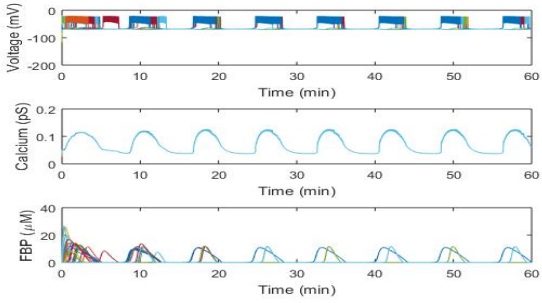

(c) Layered-split

Figure 7: CaI pairs with J_{GK} values of 0.05 and 0.14 µM·ms^{-1}, with a 3×3×3 block of cells, $g_v = 0$ pS, $g_{Ca} = 0.045$ ms^{-1}, and the initial conditions perturbed.

columns in each graph have cells with J_{GK} values all in the CaI range. The next four columns have one J_{GK} value in the CaI range and one in CaD. The last three columns have J_{GK} values both in the CaD range. These different columns are designated by dashed lines.

In Figure 8 after an hour even a small amount of calcium coupling tends to cause voltage desynchronization. We also ran the simulations for two hours and compared to the simulations for one hour, in the mixed pairs of J_{GK}, the synchronization decreases for all of the calcium coupling strengths.

We perturbed the initial conditions in Figure 9. We observe that there are some instances of desynchronization when the simulations are run for two hours instead of one hour.

4.3.2 Synchronization Trends

We can deduce from the SI plot in Figure 9, that increasing voltage coupling in the CaD mode increases synchronization in all three oscillations, voltage, calcium, and FBP. Figures 10a through 10c demonstrates the trend of synchronization as voltage increases.

Another noticeable trend drawn from Figure 9 is that in CaI mode, increasing calcium coupling increases synchronization of all three oscillations, voltage, calcium, and FBP. Figure 11 shows the increasing trend of synchronization as the strength of the calcium coupling increases.

4.3.3 Desynchronization

We observe from our the SI plot in Figure 9, that in certain cases, coupling can desynchronize the oscillations. We will compare the noticeable desynchronization cases in the following graphs.

The first desynchronization case is observed in simulations of CaD modes, where increasing calcium coupling desynchronizes voltage as seen in Figure 12.

We also see this desynchronization through the synchrony values as seen in Table 1.

SI	12a	12b
V	0.930	0.139
Ca^{2+}	0.987	0.866
FBP	0.997	0.862

Table 1: SI Values for Figures 12a and 12b

The next desynchronization case is observed when considering simulations run for two hours. Desynchronization occurs over time when both voltage and calcium were coupled and in the high end of the CaD region. In Figure 13a, calcium and FBP start to desynchronize around 40 minutes. We also see this desynchronization through the synchrony values as seen in Table 2. When we increase the calcium coupling strength in Figure 13b, the oscillations start desynchronizing around 40 minutes but re-synchronizes around 80 minutes. This is also apparent in its synchrony indices as seen in Table 3.

SI	1 hr	2 hr
Ca^{2+}	0.603	0.220
FBP	0.537	0.185

Table 2: SI Values for Figure 13a

SI	1 hr	2 hr
Ca^{2+}	0.406	0.602
FBP	0.285	0.567

Table 3: SI Values for Figure 13b

The following desynchronization case is when the FBP oscillations stop over time. We observe this case for simulations with calcium coupling only, in CaD mode of high J_{GK} values. Figure 14 demonstrates this desynchronization, where the graph of FBP oscillations become flat around 100 minutes. Note that calcium has small fast oscillations mirroring the fast spiking electrical oscillations.

5 Discussion

We used the Dual Oscillator Model and the modified ODE solver to better understand the role of calcium oscillations in CaI and CaD modes. For more examples of the trends we have observed, see reference [1]. In addition, we were able to create a synchronization index to demonstrate the trends in voltage and calcium coupling, as well as differing J_{GK} values. Through this, we were able to better study the impact of CaI, CaD, and mixed modes on oscillations. To improve simulations by modeling more cells in each simulation, the code was modified to write multiple MAT-files using a loop for a chosen time.

Coupling complex cells together has interesting dynamic effects. In CaI modes, increasing calcium coupling with no voltage coupling increases synchronization. In CaD modes, increasing voltage coupling with no calcium coupling increases synchronization as well. However, in CaD modes, voltage coupling with high calcium coupling causes desynchronization in voltage. This is reminiscent of the work on coupled cells in [16], where adding calcium

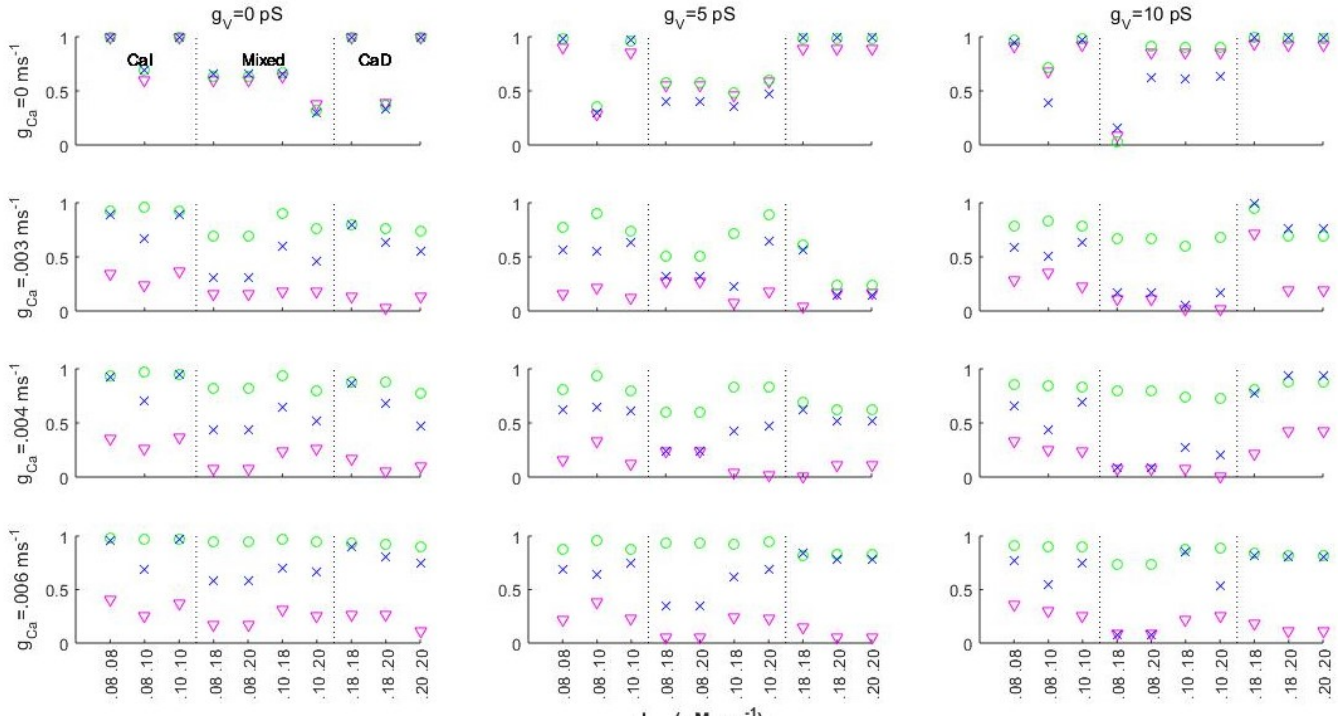

Figure 8: Simulations run with a 5×5×5 cube, the same initial conditions, and the equal-50-percent bursting pattern for one hour. V SI: ▽, Ca^{2+} SI: ◯, FBP SI: ×.

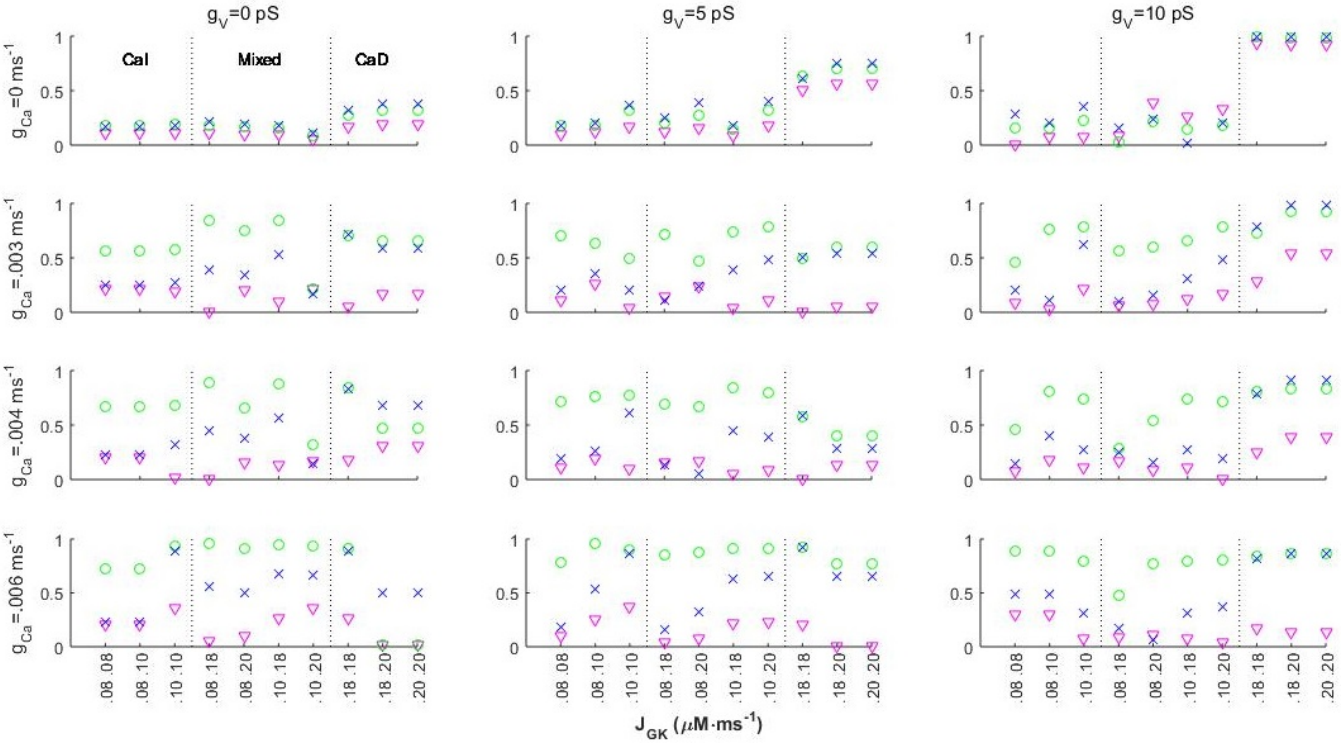

Figure 9: Simulations run for one hour with a 5×5×5 cube of cells, the equal-50-percent bursting pattern, and the initial conditions perturbed. V SI: ▽, Ca^{2+} SI: ◯, FBP SI: ×.

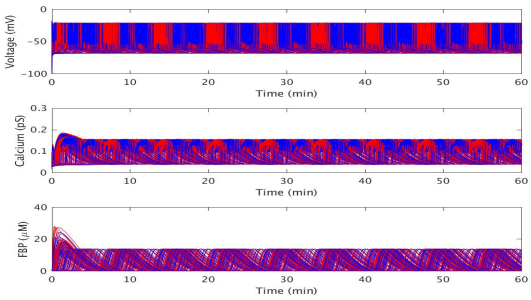

(a) $g_V = 0\,\mathrm{pS}$

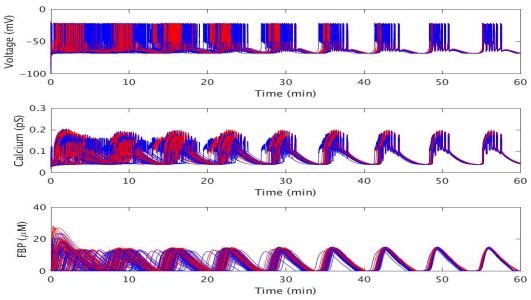

(b) $g_V = 5\,\mathrm{pS}$

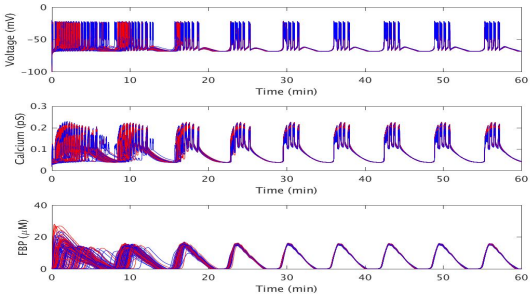

(c) $g_V = 10\,\mathrm{pS}$

Figure 10: Simulations with a 5×5×5 block of cells, $g_{Ca} = 0\,\mathrm{ms}^{-1}$, $J_{GK} = 0.18\,\mu\mathrm{M}{\cdot}\mathrm{ms}^{-1}$ (blue) or $J_{GK} = 0.20\,\mu\mathrm{M}{\cdot}\mathrm{ms}^{-1}$ (red), and the initial conditions perturbed.

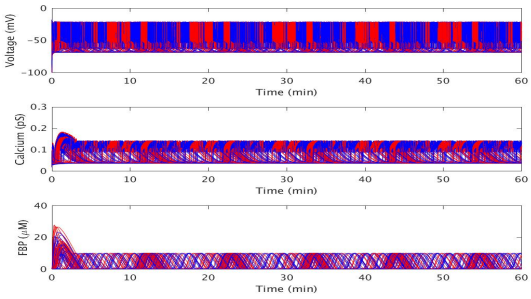

(a) $g_{Ca} = 0\,\mathrm{ms}^{-1}$

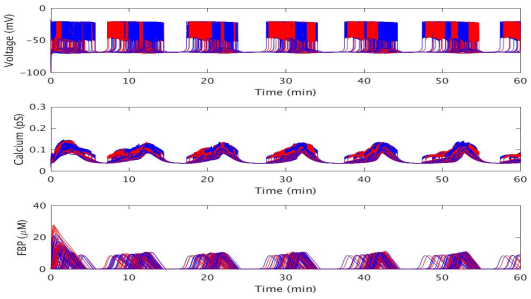

(b) $g_{Ca} = 0.0033\,\mathrm{ms}^{-1}$

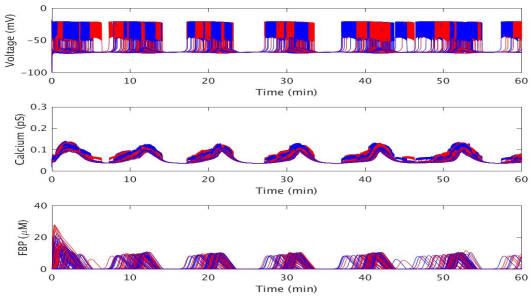

(c) $g_{Ca} = 0.006\,\mathrm{ms}^{-1}$

Figure 11: Simulations with a 5×5×5 block of cells, $g_V = 0\,\mathrm{pS}$, $J_{GK} = 0.08\,\mu\mathrm{M}{\cdot}\mathrm{ms}^{-1}$ (blue) or $J_{GK} = 0.10\,\mu\mathrm{M}{\cdot}\mathrm{ms}^{-1}$ (red), and the initial conditions perturbed.

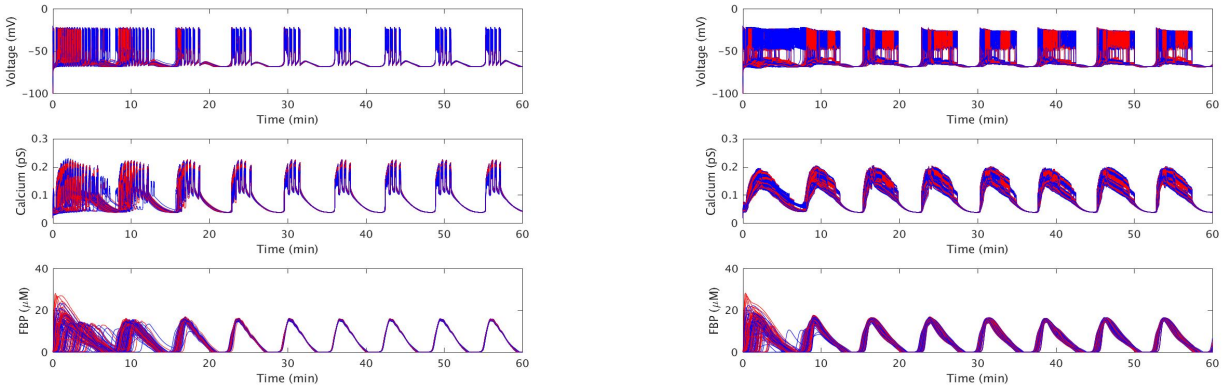

(a) $g_{Ca} = 0\,\mathrm{ms}^{-1}$ (b) $g_{Ca} = 0.006\,\mathrm{ms}^{-1}$

Figure 12: Simulations with a $5\times5\times5$ block of cells, $g_V = 10\,\mathrm{pS}$, $J_{GK} = 0.18\,\mu\mathrm{M}\cdot\mathrm{ms}^{-1}$ (blue) or $J_{GK} = 0.20\,\mu\mathrm{M}\cdot\mathrm{ms}^{-1}$ (red), and the initial conditions perturbed.

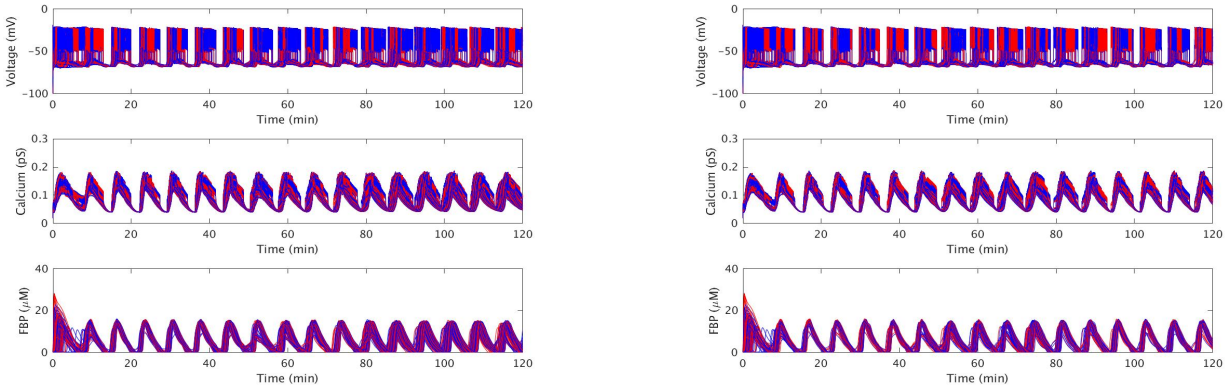

(a) $g_{Ca} = 0.003\,\mathrm{ms}^{-1}$ (b) $g_{Ca} = 0.004\,\mathrm{ms}^{-1}$

Figure 13: Simulations with a $5\times5\times5$ block of cells, $g_V = 5\,\mathrm{pS}$, $J_{GK} = 0.20\,\mu\mathrm{M}\cdot\mathrm{ms}^{-1}$ (blue and red), and the initial conditions perturbed.

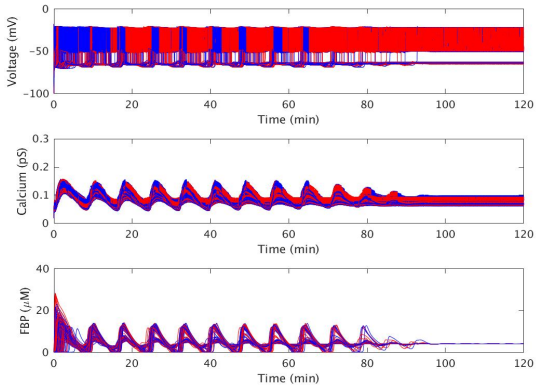

Figure 14: Simulations with a $5\times5\times5$ block of cells, $g_V = 0\,\mathrm{pS}$, $g_{Ca} = 0.004\,\mathrm{ms}^{-1}$, $J_{GK} = 0.20\,\mu\mathrm{M}\cdot\mathrm{ms}^{-1}$ (blue and red), and the initial conditions perturbed.

permeability between cells leads to a desynchronization of voltage via a pitchfork bifurcation. These results help us to better understand how calcium is organized in pancreatic islets in the process of insulin secretion.

Healthy β-cells secrete insulin in an oscillatory behavior, which occurs when cells are synchronized. High synchronization occurs when β-cells have higher voltage coupling, but a low calcium coupling according to the synchrony tables in 4.3.2. Biologically this would mean that cells synchronize more when ions are allowed to flow between them.

However further research needs to be done into the role of calcium in pancreatic β-cells. Calcium is necessary in β-cells for in sensing glucose, glycolisis, and insulin secretion. Through investigating the effects of CaD and CaI glycolytic oscillations on synchronization, we hoped to better understand its role in the β-cell. Pre-diabetic cells may have the properties of the observed desynchronization instances in 4.3.3. If identified, this will allow for the development of more precise models, which will assist in discovering anomalies in β-cells of patients with diseases such as diabetes.

Our work was limited to a single islet 125 β-cell model. This research needs to be expanded to better represent an actual pancreatic islet of Langerhans, which has thousands of cells, including α- and δ-cells, and the interaction between the many islets in a pancreas. In our tests we assumed each β-cell was coupled to all of its neighbors, which may not be the case, which could affect synchronization. Through better understating healthy, synchronized β-cells, we hope to help discover the root cause of diseases such as diabetes.

6 Acknowledgments

These results were obtained as part of the REU Site: Interdisciplinary Program in High Performance Computing (hpcreu.umbc.edu) in the Department of Mathematics and Statistics at the University of Maryland, Baltimore County (UMBC) in Summer 2016. This program is funded by the National Science Foundation (NSF), the National Security Agency (NSA), and the Department of Defense (DoD), with additional support from UMBC, the Department of Mathematics and Statistics, the Center for Interdisciplinary Research and Consulting (CIRC), and the UMBC High Performance Computing Facility (HPCF). HPCF is supported by the U.S. National Science Foundation through the MRI program (grant nos. CNS-0821258 and CNS-1228778) and the SCREMS program (grant no. DMS-0821311), with additional substantial support from UMBC. Co-author Mary Aronne was supported, in part, by the UMBC National Security Agency (NSA) Scholars Program through a contract with the NSA. Graduate assistant Janita Patwardan was supported by UMBC.

References

[1] M. Aronne, S. Clapp, S. Jung, A. Kramer, W. Wang, J. Patwardhan, and B. E. Peercy. The interaction of calcium and metabolic oscillations in pancreatic β-cells. Technical Report HPCF–2016–14, UMBC High Performance Computing Facility, University of Maryland, Baltimore County, 2016.

[2] P. Bergsten. Pathophysiology of impaired pulsatile insulin release. *Diabetes Metab. Res. Rev.*, 16:179–191, 2000.

[3] R. Bertram, L. Satin, M. Zhang, P. Smolen, and A. Sherman. Calcium and glycolysis mediate multiple bursting modes in pancreatic islets. *Biophysical Journal*, 87:3074–3087, 2004.

[4] R. Bertram, S. Satin, M. G. Pedersen, D. S. Luciani, and A. Sherman. Interaction of glycolysis and mitochondrial respiration in metabolic oscillations of pancreatic islets. *Biophysical Journal*, 92:1544–1555, 2007.

[5] P. R. Bratusch-Marrain, M. Komjati, and W. K. Waldhausl. Efficacy of pulsatile versus continuous insulin administration on hepatic glucose production and glucose utilization in type i diabetic humans. *Diabetes*, 35:922–926, 1986.

[6] G. Eskandar, J. Houser, E. Prochaska, J. Wojtkiewicz, T. Lebair, B. Peercy, M. Watts, and A. Sherman. Investigating how calcium diffusion affects metabolic oscillations and synchronization of pancreatic beta cells. *Spora: A Journal of Biomathematics*, 2:1–10, 2016.

[7] G. Eskandar, J. Houser, E. Prochaska, J. Wojtkiewicz, T. Lebair, and B.,E. Peercy. Investigating how calcium diffusion affects metabolic oscillations and synchronization of pancreatic beta cells. Technical Report HPCF–2015–24, UMBC High Performance Computing Facility, University of Maryland, Baltimore County, 2014.

[8] C. P. Fall, E. S. Marland, J. M. Wagner, and J. J. Tyson. *Computational Cell Biology*. Springer, 2002.

[9] S. Khuvis, M. K. Gobbert, and B. E. Peercy. Time-stepping techniques to enable the simulation of bursting behavior in a physiologically realistic computational islet. *Mathematical Biosciences*, 263:1–17, 2015.

[10] D. A. Lang, D. R. Matthews, M. Burnett, G. M. Ward, and R. C. Turner. Pulsatile, synchronous basal insulin and glucagon secretion in man. *Diabetes*, 31:22–26, 1982.

[11] J. Li, H. Y. Shuai, E. Gylfe, and A. Tengholm. Oscillations of sub-membrane atp in glucose-stimulated beta cells depend on negative feedback from ca^{2+}. *Diabetologia*, 56:1577–1586, 2013.

[12] D. R. Matthews, B. A. Naylor, R. G. Jones, G. M. Ward, and R. C. Turner. Pulsatile insulin has greater hypoglycemic effect than continuous delivery. *Diabetes*, 32:617–621, 1983.

[13] G. Paolisso, S. Sgambato, R. Torella, M. Varricchio, A. Scheen, F. D'Onofrio, and P. J. Lefebvre. Pulsatile insulin delivery is more efficient than continuous infusion in modulating islet cell function in normal subjects and patients with type 1 diabetes. *J. Clin. Endocrinol Metlab*, (66):1220–1226, 1998.

[14] N. Porksen. The in vivo regulation of pulsatile insulin secretion. *Diabetologia*, 45:3–20, 2002.

[15] S. H. Song, L. Kjems, R. Ritzel, S. M. McIntyre, M. L. Johnson, J. D. Veldhuis, and P. C. Butler. Pulsatile insulin secretion by human pancreatic islets. *J. Clin. Endocrinal. Metab*, 87:213–221, 2002.

[16] K. Tsaneva-Atanasova, C. L. Zimliki, R. Bertram, and A. Sherman. Diffusion of calcium and metabolites in pancreatic islets: killing oscillations with a pitchfork. *Biophysical Journal*, 90:3434–3046, 2006.

[17] M. Watts, B. Fendler, M. J. Merrins, L. S. Satin, R. Bertram, and A. Sherman. Calcium and metabolic oscillations in pancreatic islets: Who's driving the bus? *SIAM Journal on Applied Dynamical Systems*, 13(2):683–703, 2014.

[18] M. Zhang, B. Fendler, B. Peercy, P. Goel, R. Bertram, A. Sherman, and L. Satin. Long lasting synchronization of calcium oscillations by cholinergic stimulation in isolated pancreatic islets. *Biophysical Journal*, 95:4676–4688, 2008.